

Electronic Supplementary Information

A Dithieno[3,2-b:2',3'-d]pyrrole Cored Four-Arm Hole Transporting Material for Over 19% Efficiency Dopant-Free Perovskite Solar Cells

Zihao Dong,^a Xinxing Yin,^a Amjad Ali,^a Jie Zhou,^a Sandip Singh Bista,^b Cong Chen,^b
Yanfa Yan*^b and Weihua Tang*^a

Zihao Dong, Xinxing Yin, Amjad Ali, Dr. Jie Zhou, Prof. Weihua Tang
School of Chemical Engineering, Nanjing University of Science and Technology,
Nanjing, 210094, China
E-mails: whtang@njust.edu.cn;

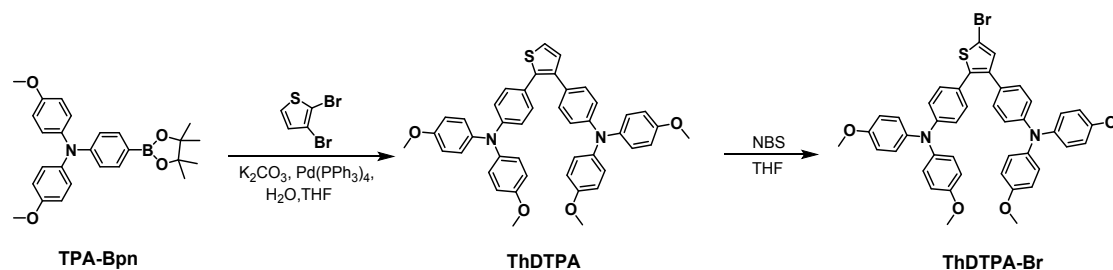
Sandip Singh Bista, Cong Chen, Prof. Yanfa Yan
Department of Physics and Astronomy and Wright Center for Photovoltaics Innovation
and Commercialization, The University of Toledo, Toledo, OH 43606, United States
E-mail: yanfa.yan@utoledo.edu

Table of Content

1. Synthesis and characterization of HTMs.....	2
2. Instruments and general methods.....	7
3. Quantum chemistry calculations.....	8
4. Device fabrication.....	9
5. Electrochemical properties.....	12
6. Hole-transporting properties.....	12
7. Dopant-free HTMs for PVSCs over 18% efficiency Summary.....	13

1. Synthesis and characterization of HTMs

All commercially available chemicals were purchased from J&K (Shanghai, China) and used as received without further purification. The solvents were freshly distilled prior to use. The synthesis of distannylated 4-octyl-4H-dithieno[3,2-*b*:2',3'-*d*]pyrrole (DTPC8-tin) were carried out referring to previous literatures.^{1,2}



Scheme S1. Synthetic route of ThDTPA-Br.

Synthesis of 4,4'-(thiophene-2,3-diyl)bis(N,N-bis(4-methoxyphenyl)aniline) (ThDTPA)

The solution of 2,3-dibromothiophene (880 mg, 3.64 mmol), TPA-BPn (3.45 g, 8.00 mmol) and potassium carbonate (5 mL, 2.0 M in deionized water) in freshly distilled toluene (20 mL) was degassed with nitrogen for 0.5 h. Pd(PPh₃)₄ (210 mg, 0.18 mmol) was then quickly added into the mixture under the protection of nitrogen. The mixture was heated to reflux overnight until no 2,3-dibromothiophene was detected by TLC. The resulting mixture was extracted with dichloromethane, washed with water and dried with MgSO₄. After removal of solvent, the residue was purified by column chromatography (silica gel, petroleum ether/dichloromethane, v/v, 1/1) to afford ThDTPA as an aqua solid (2.3 g, 91 %). ¹H NMR (500 MHz, CDCl₃): 7.22-7.08 (m, 14H), 6.86–6.84 (m, 12H), 3.81 (s, 12H); ¹³C NMR (125 MHz, CDCl₃): 156.10, 155.97, 147.97, 147.46, 140.75, 137.99, 137.03, 130.53, 130.48, 129.82, 129.66, 128.93, 126.97, 126.42, 123.09, 123.02, 120.16, 119.74, 114.80, 55.59.

Synthesis of 4,4'-(5-bromothiophene-2,3-diyl)bis(N,N-bis(4-methoxyphenyl)aniline) (ThDTPA-Br)

Toward the solution of ThDTPA (2.26 g, 3.27 mmol) and *p*-toluenesulfonic acid (563 mg, 3.27 mmol) in freshly distilled THF (15 mL) at 0 °C was added NBS (640 mg, 3.60 mmol) in three portions. The mixture was quenched with water after 2 h. The organic phase was extracted with dichloromethane and dried with MgSO₄. After removal of solvent, the crude product residue was purified by column chromatography (silica gel, petroleum ether/dichloromethane, v/v, 1/1) to afford ThDTPA-Br as aqua solid (2.2 g, 87 %). ¹H NMR (500 MHz, CDCl₃): 7.11–7.06 (m, 13H), 6.87–6.80 (m, 12H), 3.82 (s, 12H); ¹³C NMR (125 MHz, CDCl₃): 156.01, 155.81, 148.09, 147.54, 140.59, 140.29, 139.10, 137.17, 132.76, 129.43, 129.27, 127.33, 126.89, 126.65, 124.90, 119.62, 119.16, 114.62, 114.57, 109.30, 55.33.

Synthesis of 4,4'-((4-octyl-4H-dithieno[3,2-b:2',3'-d]pyrrole-2,6-diyl)bis(thiophene-5,2-diyl))bis(N,N-bis(4-methoxyphenyl)aniline) (DTPC8-ThDTPA)

The solution of DTPC8-tin (400 mg, 0.46 mmol) and ThDTPA-Br (994 mg, 1.16 mmol) in toluene (15 mL) was degassed with nitrogen for 0.5 h, then it was added with Pd(PPh₃)₄ (30 mg, 0.02 mmol). The mixture was refluxed until no DTPC8-tin was detected by TLC. After cooling to room temperature, the mixed solution was evaporated under reduced pressure. DTPC8-ThDTPA (700 mg, 80 %) was recrystallized to obtain a dark red solid by column chromatography (silica gel, petroleum ether/ethyl acetate, v/v, 3/1). ¹H NMR (500 MHz, CDCl₃): 7.18–7.15 (m, 8H), 7.09–7.08 (m, 18H), 6.88–6.80 (m, 26H), 4.16 (s, 2H), 3.81 (s, 24H), 1.89–1.88 (m, 2H), 1.35–1.27 (m, 10H), 0.88–0.86 (t, *J* = 5 Hz, 3H); ¹³C NMR (125 MHz, CDCl₃): 156.19, 155.99, 148.04, 147.71, 144.77, 141.01, 140.70, 137.80, 136.44, 135.82, 135.15, 129.63, 129.54, 128.70, 127.98, 127.05, 126.81, 126.61, 126.43, 125.99, 120.16, 119.61, 114.85, 114.81, 114.71, 114.05, 107.03, 55.62, 47.53, 31.94, 30.47, 29.36, 29.30, 27.14, 22.76, 14.23. MALDI-TOF MS: *m/z* = 1667.5908 [M]⁺, calcd. for C₁₀₄H₉₃N₅O₈S₄: 1667.5907.

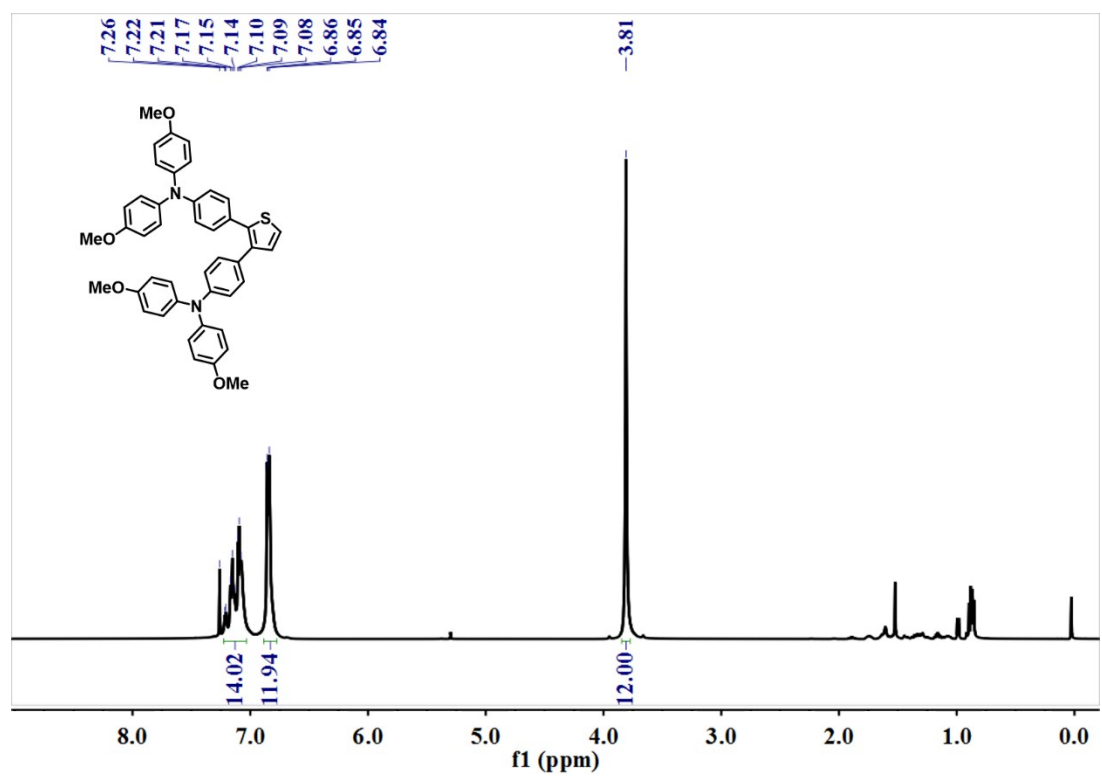


Fig. S1. ¹H NMR spectrum of ThDTPA.

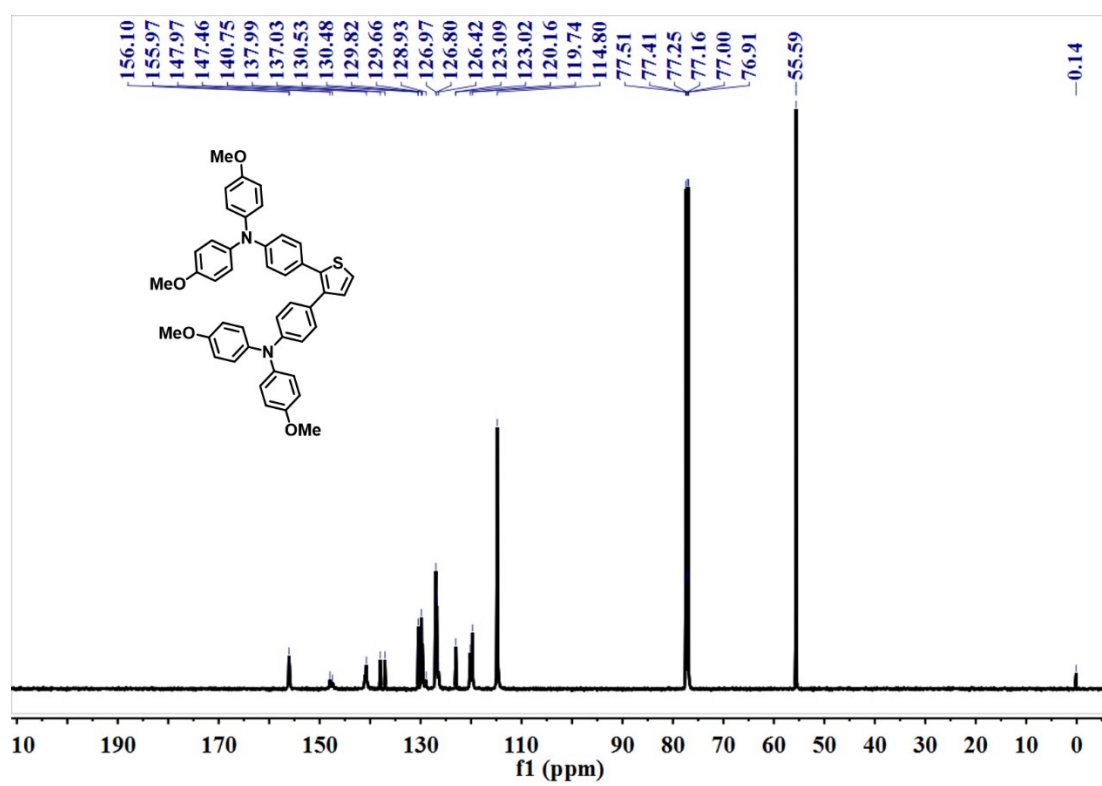


Fig. S2. ¹³C NMR spectrum of ThDTPA.

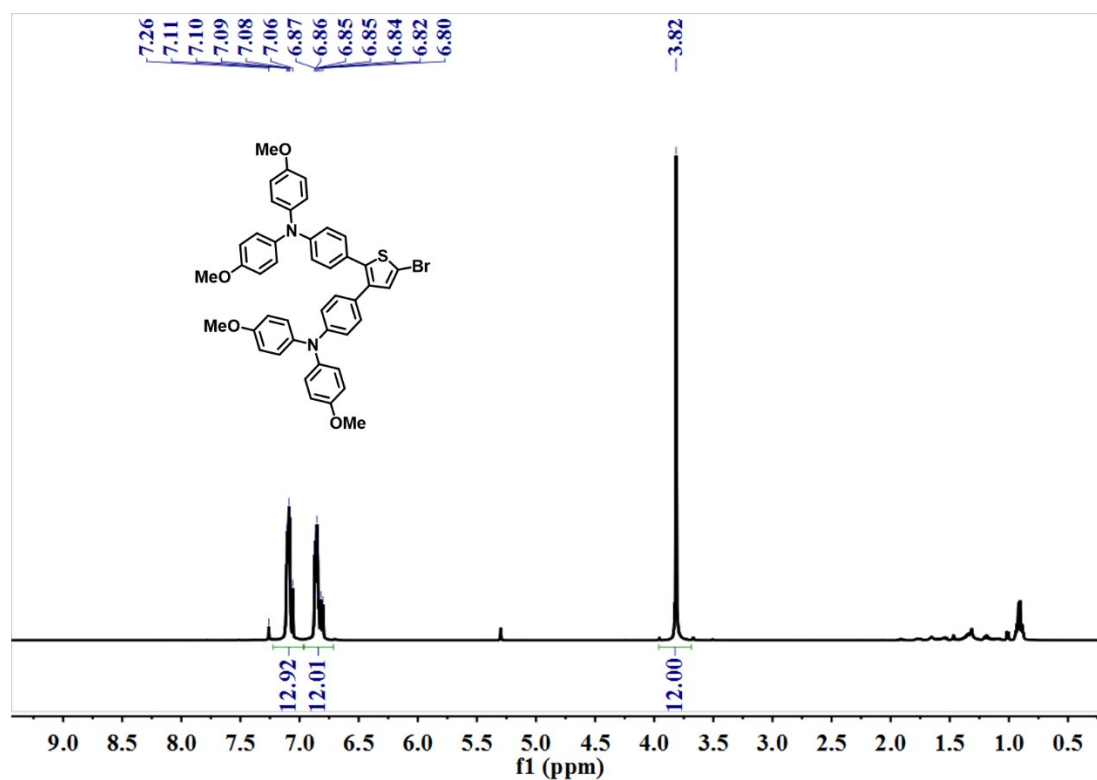


Fig. S3. ^1H NMR spectrum of ThDTPA-Br.

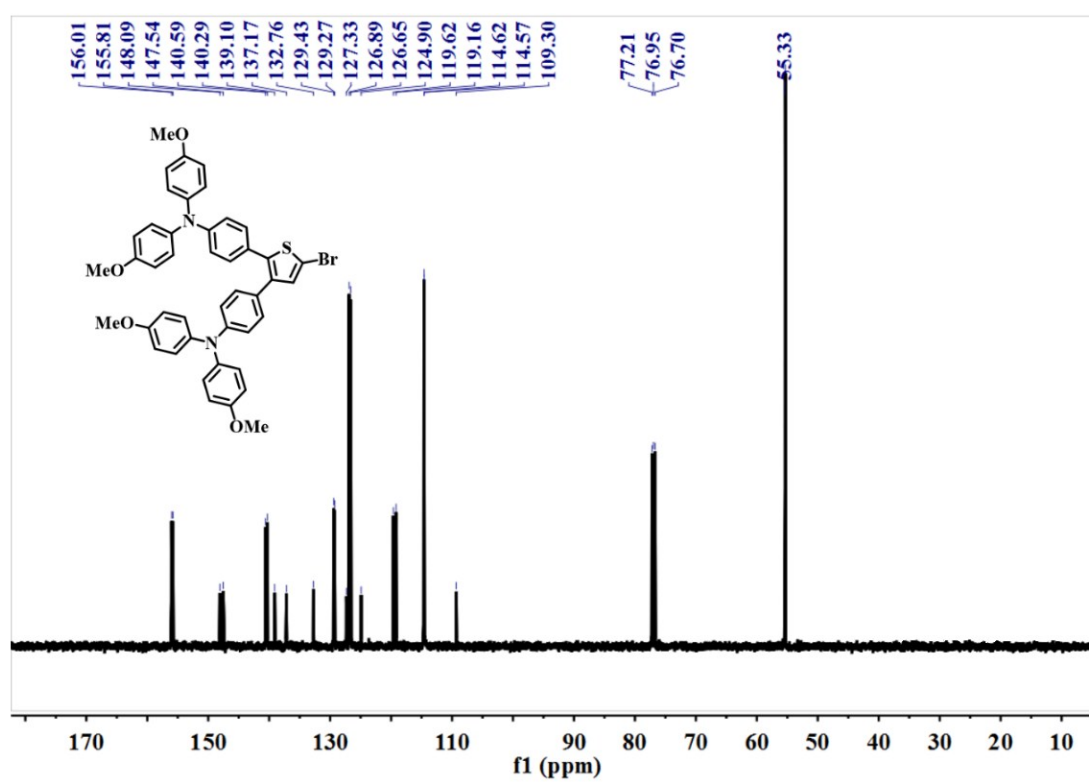


Fig. S4. ^{13}C NMR spectrum of ThDTPA-Br.

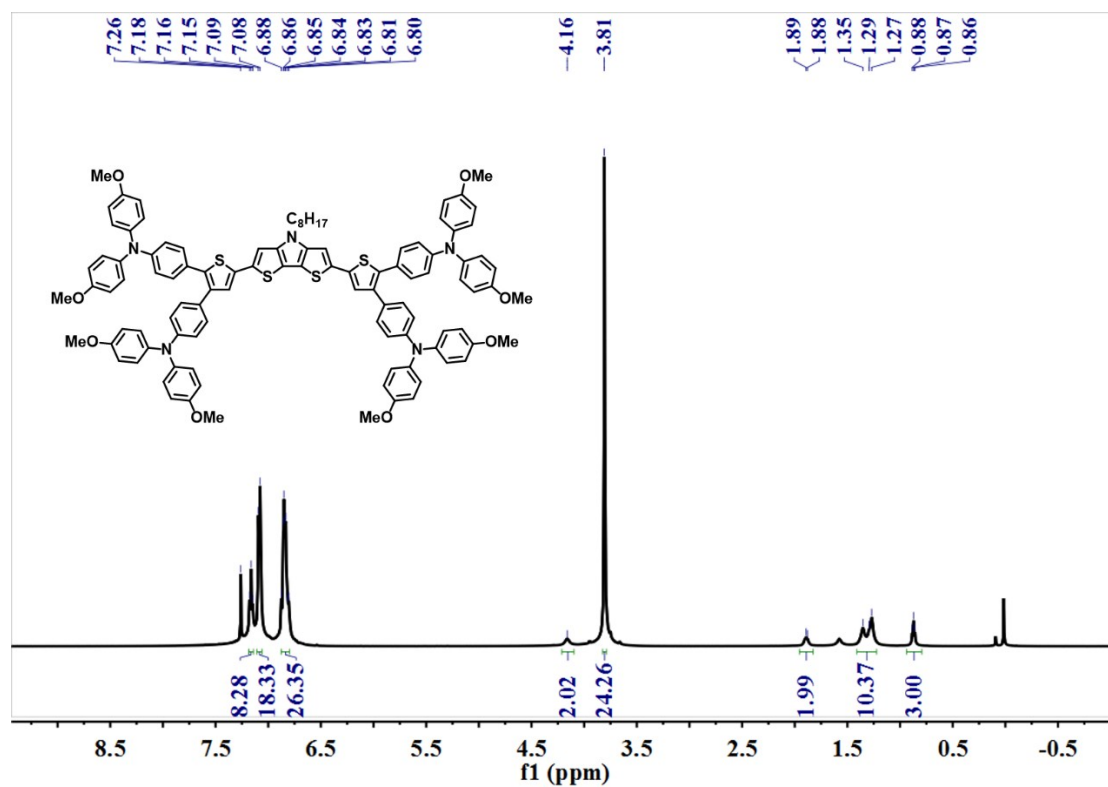


Fig. S5. ¹H NMR spectrum of DTPC8-ThDTPA.

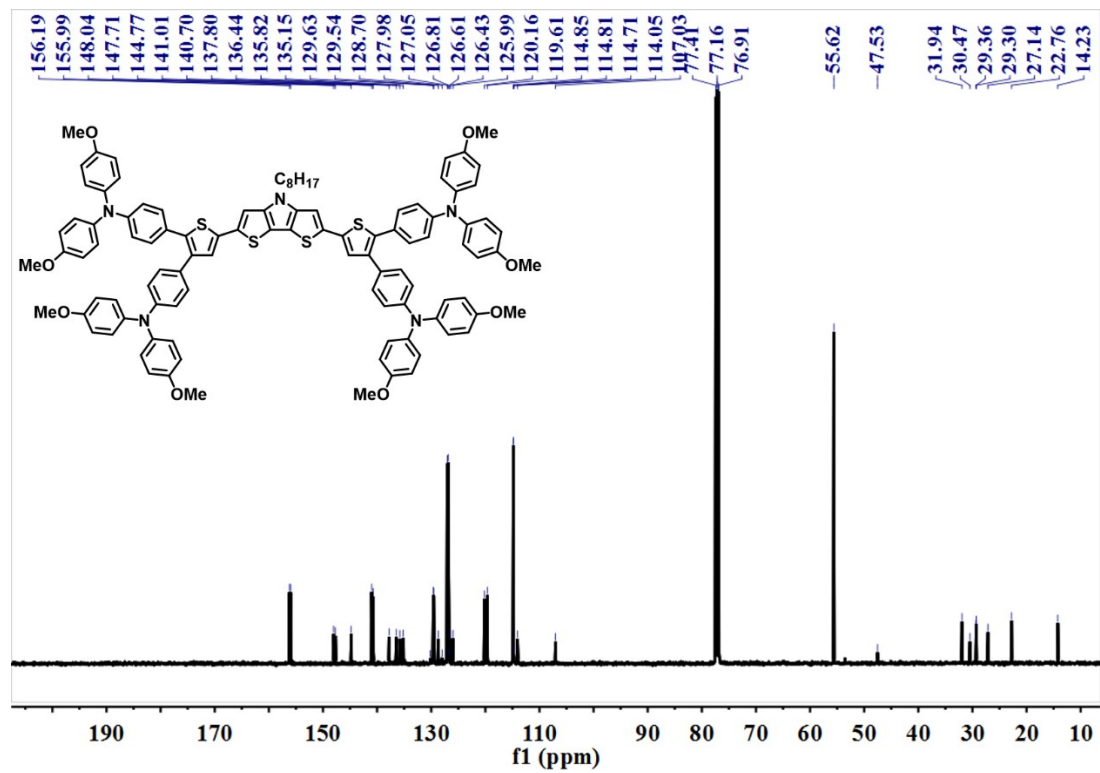


Fig. S6. ¹³C NMR spectrum of DTPC8-ThDTPA.

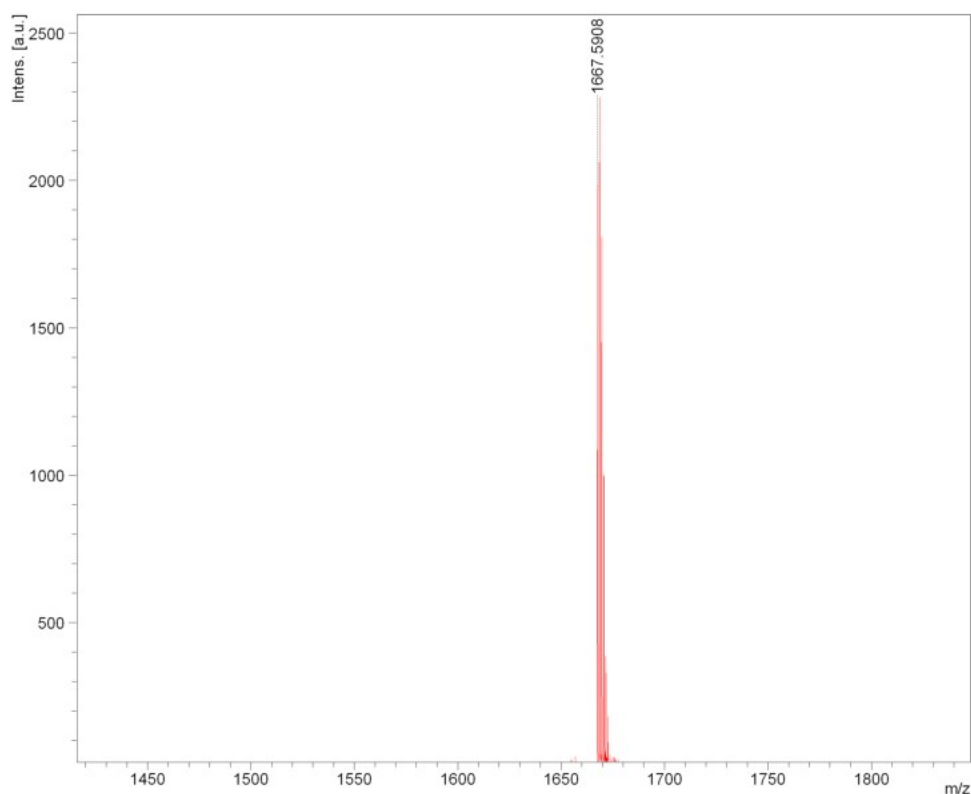


Fig. S7. MALDI-TOF spectrum of DTPC8-ThDTPA.

2. Instruments and general methods

The ^1H and ^{13}C NMR spectra were recorded on Bruker AVANCE III with tetramethylsilane (TMS) as standard substance. Mass spectra were obtained by Bruker ultrafleXtreme MALDI TOF/TOF. The absorption spectra were measured on a UV-Vis spectrophotometer (Evolution 220, Thermo Fisher). Photoluminescence (PL) spectrum was conducted on Horiba Jobin Yvon Model FM-4NIR spectrophotometer. Thermogravimetric analysis (TGA) was conducted under nitrogen atmosphere at a heating rate of $20\text{ }^\circ\text{C min}^{-1}$ from $50\text{ }^\circ\text{C}$ to $800\text{ }^\circ\text{C}$. The instrument type was TGA/SDTA851E (Mettler Toledo). Decomposition temperature (T_g) was defined with 5 % weight loss. Differential Scanning Calorimeter (DSC) was conducted on PerkinElmer Thermal Analysis at a scan rate of $10\text{ }^\circ\text{C min}^{-1}$ from $50\text{ }^\circ\text{C}$ to $250\text{ }^\circ\text{C}$. The electrochemical cyclic voltammetry (CV) was conducted on an electrochemical workstation (CHI760D Chenhua, Shanghai) with Pt plate as working electrode, Pt slice as counter electrode, and Ag/AgCl electrode as reference electrode in

tetrabutylammonium hexafluorophosphate (*n*-Bu₄NPF₆, 0.1 M) dichloromethane solutions at a scan rate of 50 mV s⁻¹. With the use of ferrocene as internal standard, the HOMO energy level was calculated from the onset oxidation (E_{onsetox}) as $\text{HOMO} = - (E_{\text{onset}} + 4.8 \text{ eV})$;⁴ while the LUMO energy level was calculated with HOMO and optical bandgap (E_g) by the equation as: $\text{LUMO} = \text{HOMO} + E_g \text{ (eV)}$. The UPS spectra were measured using HeI 21.22 eV as the excitation source with an energy resolution of 0.05 eV to investigate the work function and the frontier electronic structure features. The work function was derived from the secondary electron cutoff of the spectra, and the ionization potential is estimated from the frontier edge of the occupied density of states.

3. Quantum chemistry calculations

Density functional theory (DFT) calculation is used for evaluating molecule characteristics at B3LYP/6-31G(d,p) level using Gaussian 09 program suite.⁵ Chemical structural optimization and subsequent frequency calculations are performed for the ground state using an all electron popple double zeta basis set with one polarization function on heavy atoms (non-hydrogen atoms like C, N, O and S etc.) and one on H atom (6-31G(d, p)). The hole reorganization energy (λ) was calculated by $\lambda_h = E^+(\text{N}) - E^+(\text{C}) + E(\text{C}) - E(\text{N})$,⁶ where $E^+(\text{N})$, $E^+(\text{C})$, $E(\text{C})$ and $E(\text{N})$ for DTTPC8-ThDTPA are calculated to be -6487.2550, -6487.2585, -6487.4334, -6487.4348 hartree, respectively.

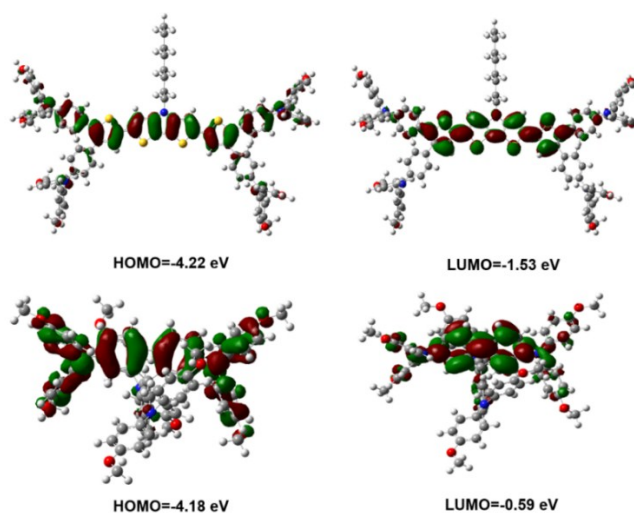


Fig. S8. Calculated $E_{\text{HOMO}}/E_{\text{LUMO}}$ energy levels for DTTPC8-ThDTPA (top) and spiro-OMeTAD (bottom).

4. Device fabrication

Methylammonium iodide (MAI, Dyesol), formamidinium iodide (FAI, Dyesol), lead iodide (PbI₂, Alfa Aesar), lead bromide (PbBr₂, TCI), lead thiocyanate (Pb(SCN)₂, Sigma-Aldrich, 99.5%), dimethylsulfoxide (DMSO, Sigma-Aldrich) and *N,N*-dimethylformamide (DMF, Sigma-Aldrich) were used as received without further purification.

Preparation of perovskite (MA_{0.7}FA_{0.3}PbI_{2.85}Br_{0.15}) precursor solution:

The solution was prepared using a Lewis acid-base adduct approach with the mixture of MAI (0.7 mmol), FAI (0.3 mmol), PbI₂ (0.925 mmol), PbBr₂ (0.075 mmol), DMSO (71 μL) and Pb(SCN)₂ (9.22 mg) in DMF (600 μL). The resulted precursor was stirred at 60 °C and then purified using a 0.45 μm filter before spin-coating.

Preparation of HTMs solution:

DTPC8-ThDTPA (10 mg) was dissolved in dry chlorobenzene (1 mL) without additives. The spiro-OMeTAD solution was prepared by dissolving 72.3 mg spiro-OMeTAD (Shenzhen Feiming Science and Technology Co., Ltd.) in 1 mL chlorobenzene with 28 μL 4-*tert*-butylpyridine (*t*-BP) (Sigma-Aldrich), 18 μL Li-TFSI (520 mg mL⁻¹ in acetonitrile, Sigma-Aldrich) and 18 μL Co(III)-TFSI salt (FK102, 300 mg mL⁻¹ in acetonitrile, Dyesol).

Device fabrication:

The FTO glass was fully washed off in order by diluted detergent, DI water, acetone and isopropanol for 30 minutes ultrasound treatment. The SnO₂ layer was deposited on clean FTO with plasma-enhanced atomic layer deposition (PEALD) method, the thickness was around 15 nm. The SnO₂ layer was annealed at 100 °C for 1 h in ambient air and the humidity was around 55%. Then it was treated with ultraviolet ozone (UV-Ozone) for 20 minutes and transferred to a nitrogen-filled glove box. Subsequently, a solution of C₆₀-SAM (4 mg mL⁻¹) in chlorobenzene was spin-coated on the PEALD SnO₂ layer at a speed of 3000 rpm for 1 minute. The perovskite precursor solution was then spin-coated on the SnO₂ layer at 500 rpm for 3 s and at 4000 rpm for 60 s using

diethyl ether as anti-solvent agent, 700 μL diethyl ether was dropped onto the perovskite surface at 55 s before end in one portion. The perovskite layer was annealed at 100 $^{\circ}\text{C}$ for 5 min after spin coating. The PMMA (1 mg mL^{-1} in chlorobenzene) passivation layer was spin coated on the top of the perovskite film at a speed of 6000 rpm, then annealed at 100 $^{\circ}\text{C}$ for 10 minutes. HTMs solution was spin-coated on the perovskite film at 3000 rpm for 1 minute, resulting a ~ 40 nm layer. Finally, a layer of 80 nm gold cathode was deposited on the HTM layer using thermal evaporation. The working area of the devices was 0.08 cm^2 as defined by a shadow mask during the Au evaporation.

Hole mobility measurements:

With the hole-only device structure of ITO/PEDOT:PSS/HTMs/MoO₃/Ag, the charge transport behavior of two HTMs was measured using the space-charge-limited current (SCLC). HTMs under a concentration of 20 mg mL^{-1} in anhydrous chloroform were spin-coated on PEDOT:PSS at 3000 rpm. The thickness of HTMs is around 100 nm. A double-layer cathode configuration of MoO₃(5 nm)/Ag(80 nm) was spined covering on the top of the HTM layer. The measured voltage range was from -10 V to 10 V.

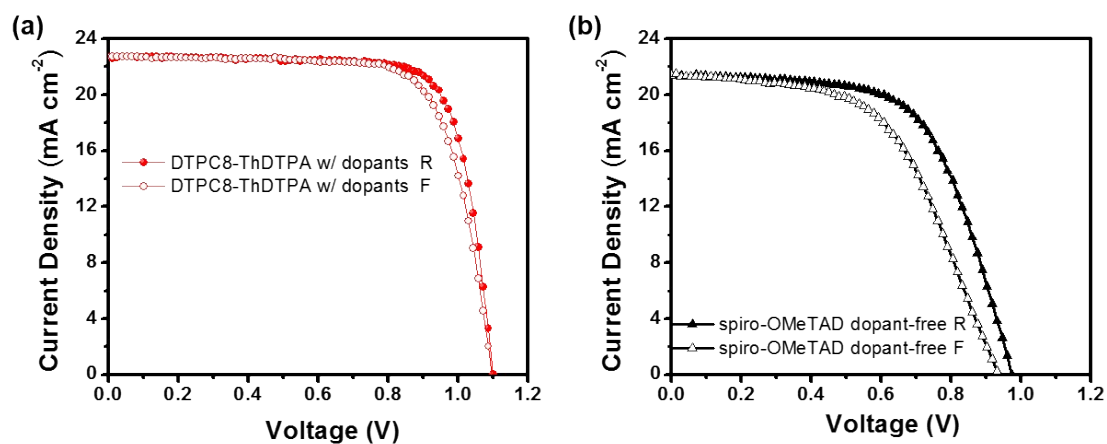


Fig. S9. J - V curves under 100 mW cm^{-2} AM1.5G illumination of PVSCs for (a) DTPC8-ThDTPA with dopants and (b) dopant-free spiro-OMeTAD.

Table S1. Photovoltaic performances of PVSCs for DTPC8-ThDTPA with dopants and dopant-free spiro-OMeTAD HTMs under AM1.5G illumination (100 mW cm^{-2}).

HTMs	Scan direction	V_{oc} [V]	J_{sc} [mA cm^{-2}]	FF	PCE [%]
DTPC8-ThDTPA with dopants	reverse	1.094	22.70	0.773	19.20
	forward	1.089	22.72	0.738	18.26
Dopant-free spiro-OMeTAD	reverse	0.973	21.41	0.616	12.83
	forward	0.935	21.39	0.545	10.90

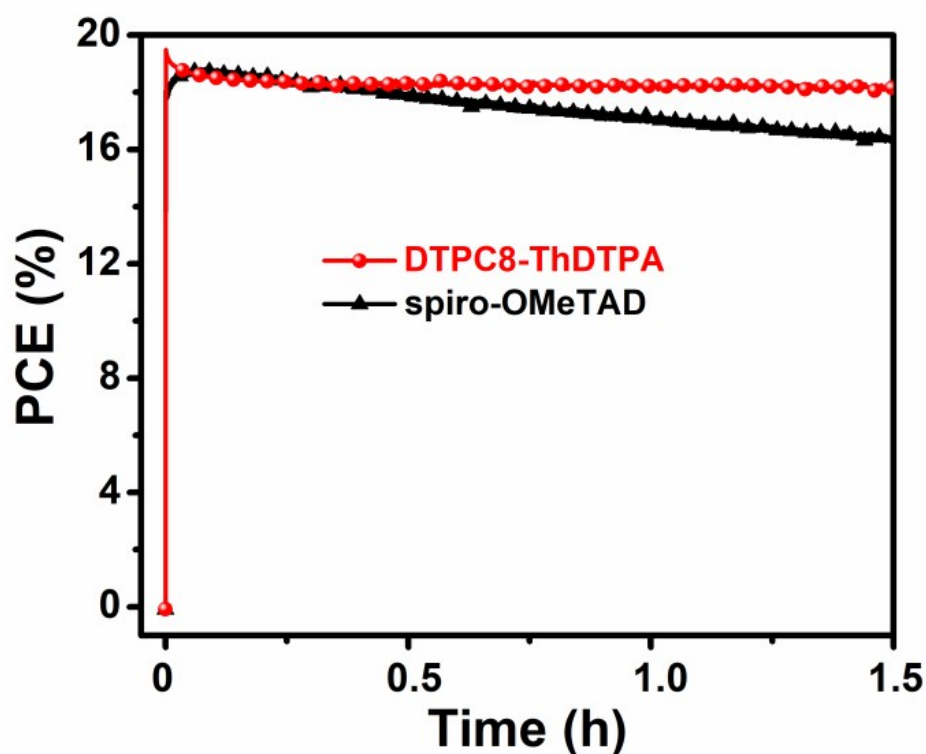


Fig. S10. Steady-state efficiency (1.5 h 100 mW cm^{-2} AM1.5G illumination) of the best-performing PVSC for DTPC8-ThDTPA and spiro-OMeTAD.

5. Electrochemical properties

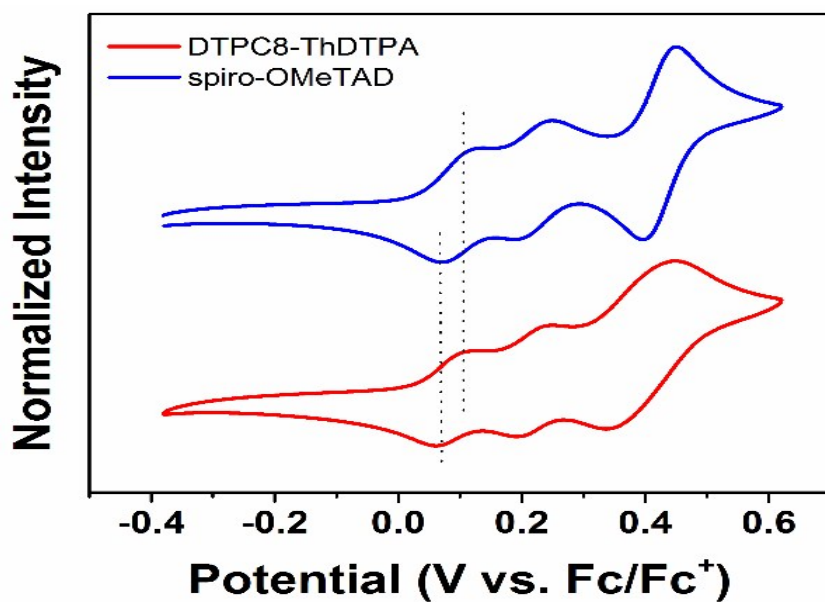


Fig. S11. CV curves of DTPC8-ThDTPA and spiro-OMeTAD in CH₂Cl₂ solution.

6. Hole-transporting properties

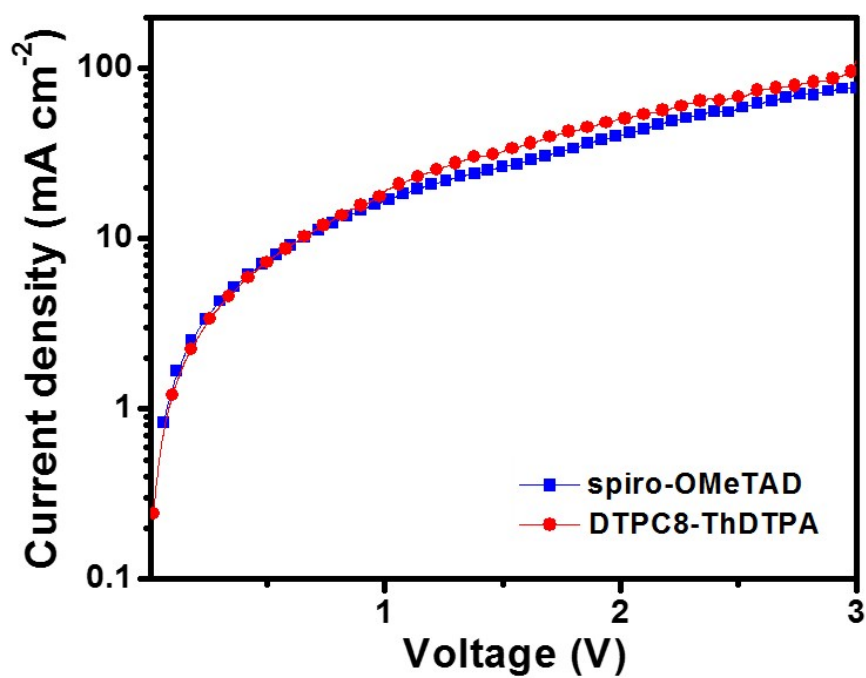


Fig. S12. SCLC hole-mobility curves of un-doped DTPC8-ThDTPA (~40 nm) and spiro-OMeTAD (~150 nm).

7. Dopant-free HTMs for PVSCs over 18% efficiency Summary

Table S2. Dopant-free HTMs for PVSCs over 18% efficiency summary.

HTM	perovskite	Doped spiro-OMeTAD PCE/%	PCE /%	Reference
ICTH2	MAPbI ₃	14.74	18.75	7
mDPA-DBTP	MAPbI ₃	17.82	18.09	8
PCA-1	Mesoscopic MAPbI ₃	18.30	18.17	9
BTF4	(FAPbI ₃) _{0.85} (MAPbBr ₃) _{0.15}	-	18.03	10
KR321	(FAPbI ₃) _{0.85} (MAPbBr ₃) _{0.15}	19.01	19.03	11
Trux-OMeTAD	MAPbI ₃	-	18.6	12
TTE-2	(FAPbI ₃) _{0.95} (MAPbBr ₃) _{0.05}	-	20.04	13
m-MTDATA	Cs _{0.05} (FA _{0.85} MA _{0.15}) _{0.95} Pb(I _{0.85} Br _{0.15}) ₃	-	18.12	14
TAPC	MAPbI ₃	-	18.80	15
FBA3	MAPbI _x Cl _{3-x}	17.57	19.27	16
FMT	MAPbI ₃	-	19.06	17
DTPC8-ThDTPA	MA_{0.7}FA_{0.3}PbI_{2.85}Br_{0.15}	19.59	19.42	our report

8. PL spectra

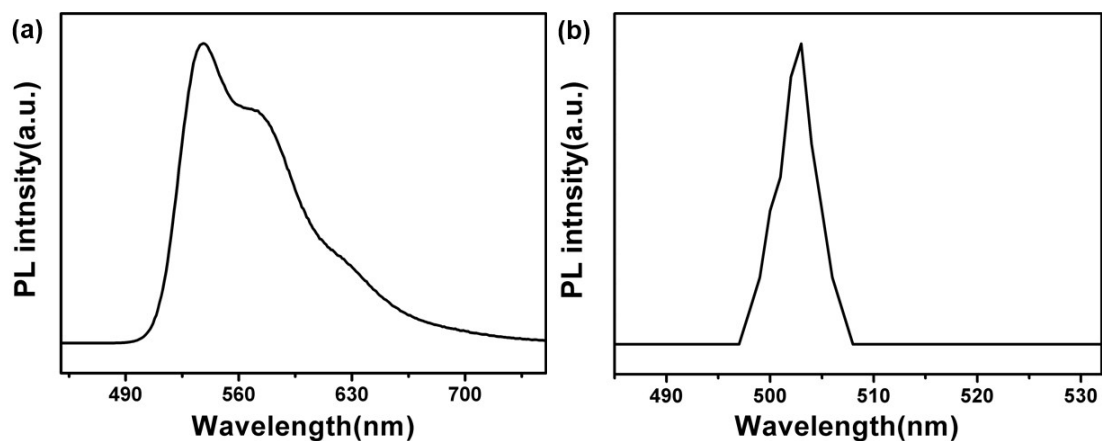


Fig. S13. PL spectra of a DTPC8-ThDTPA in solution(a) and film(b).

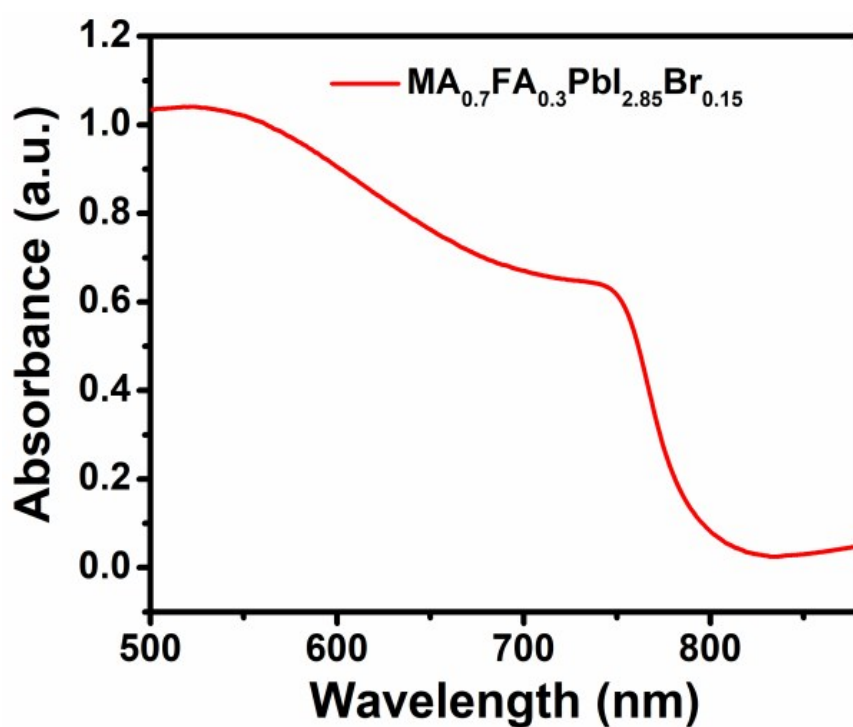


Fig. S14. PL spectra of $\text{MA}_{0.7}\text{FA}_{0.3}\text{PbI}_{2.85}\text{Br}_{0.15}$ perovskite film.

Reference

- 1 M. C. Sil, M. F. M. Kavungathodi, J. Nithyanandhan, *Dyes Pigments*, 2019, **161**, 313-323.
- 2 J. Sun, X. Ma, Z. Zhang, J. Yu, J. Zhou, X. Yin, L. Yang, R. Geng, R. Zhu, F. Zhang, W. Tang, *Adv. Mater.*, 2018, **30**, 1707150.

- 3 X. Yin, L. Guan, J. Yu, D. Zhao, C. Wang, N. Shrestha, Y. Han, Q. An, J. Zhou, B. Zhou, Y. Yu, C. R. Grice, R. A. Awni, F. Zhang, J. Wang, R. J. Ellingson, Y. Yan, W. Tang, *Nano Energy*, 2017, **40**, 163.
- 4 B. Xu, J. Zhang, Y. Hua, P. Liu, L. Wang, C. Ruan, Y. Li, G. Boschloo, E. M. J. Johansson, L. Kloo, A. Hagfeldt, A. K. Y. Jen, L. Sun, *Chem*, 2017, **2**, 676.
- 5 M. J. Frisch, G. W. Trucks, H. B. Schlegel, G. E. Scuseria, M. A. Robb, J. R. Cheeseman, G. Scalmani, V. Barone, B. Mennucci, G. A. Petersson, H. Nakatsuji, M. Caricato, X. Li, H. P. Hratchian, A. F. Izmaylov, J. Bloino, G. Zheng, J. L. Sonnenberg, M. Hada, M. Ehara, K. Toyota, R. Fukuda, J. Hasegawa, M. Ishida, T. Nakajima, Y. Honda, O. Kitao, H. Nakai, T. Vreven, J. A. Montgomery, J. E. Peralta, F. Ogliaro, M. Bearpark, J. J. Heyd, E. Brothers, K. N. Kudin, V. N. Staroverov, T. Keith, R. Kobayashi, J. Normand, K. Raghavachari, A. Rendell, J. C. Burant, S. S. Iyengar, J. Tomasi, M. Cossi, N. Rega, J. M. Millam, M. Klene, J. E. Knox, J. B. Cross, V. Bakken, C. Adamo, J. Jaramillo, R. Gomperts, R. E. Stratmann, O. Yazyev, A. J. Austin, R. Cammi, C. Pomelli, J. W. Ochterski, R. L. Martin, K. Morokuma, V. G. Zakrzewski, G. A. Voth, P. Salvador, J. J. Dannenberg, S. Dapprich, A. D. Daniels, O. Farkas, J. B. Foresman, J. V. Ortiz, J. Cioslowski, D. J. Fox, Gaussian, Inc., Wallingford CT, 2013.
- 6 J. Yin, R.-F. Chen, S.-L. Zhang, H.-H. Li, G.-W. Zhang, X.-M. Feng, Q.-D. Ling, W. Huang, *J. Phys. Chem. C*, 2011, **115**, 14778.
- 7 D. Bharath, M. Sasikumar, N. R. Chereddy, J. R. Vaidya, S. Pola, *Sol. Energy*, 2018, **174**, 130-138.
- 8 R. Azmi, S. Y. Nam, S. Sinaga, Z. A. Akbar, C.-L. Lee, S. C. Yoon, I. H. Jung, S.-Y. Jang, *Nano Energy*, 2018, **44**, 191-198.
- 9 Y. Li, K. R. Scheel, R. G. Clevenger, W. Shou, H. Pan, K. V. Kilway, Z. Peng, *Adv. Energy Mater.*, 2018, **8**, 1801248.
- 10 X. Sun, Q. Xue, Z. Zhu, Q. Xiao, K. Jiang, H. L. Yip, H. Yan, Z. Li, *Chem. Sci.*, 2018, **9**, 2698.
- 11 K. Rakstys, S. Paek, P. Gao, P. Gratia, T. Marszalek, G. Grancini, K. T. Cho, K. Genevicius, V. Jankauskas, W. Pisula, M. K. Nazeeruddin, *J. Mater. Chem. A*, 2017, **5**, 7811–7815.

- 12 C. Huang, W. Fu, C. Z. Li, Z. Zhang, W. Qiu, M. Shi, P. Heremans, A. K. Y. Jen and H. Chen, *J. Am. Chem. Soc.*, 2016, **138**, 2528–2531.
- 13 C. Shen, Y. Wu, H. Zhang, E. Li, W. Zhang, X. Xu, W. Wu, H. Tian, W. H. Zhu, *Angew. Chem. Int. Ed.*, 2019, **58**, 3784-3789.
- 14 R. Chen, T. Bu, J. Li, W. Li, P. Zhou, X. Liu, Z. Ku, J. Zhong, Y. Peng, F. Huang, Y.-B. Cheng and Z. Fu, *ChemSusChem*, 2018, **11**, 1467-1473.
- 15 L. Yang, F. Cai, Y. Yan, J. Li, D. Liu, A. J. Pearson and T. Wang, *Adv. Funct. Mater.*, 2017, **27**, 1702613.
- 16 X. Sun, F. Wu, C. Zhong, L. Zhu and Z. a. Li, *Chemical Science*, 2019, DOI: 10.1039/c9sc01697j.
- 17 J. Zhang, Q. Sun, Q. Chen, Y. Wang, Y. Zhou, B. Song, N. Yuan, J. Ding and Y. Li, *Adv. Funct. Mater.*, 2019, **29**, 1900484.